

Conformational Preferences of Neurotransmitters: Ephedrine and Its Diastereoisomer, Pseudoephedrine

Patrick Butz,[†] Romano T. Kroemer,[‡] Neil A. Macleod,[†] and John P. Simons^{*,†}

Physical and Theoretical Chemistry Laboratory, University of Oxford, South Parks Road, Oxford OX1 3QZ, United Kingdom, and Department of Chemistry, Queen Mary and Westfield College, University of London, Mile End Road, London E1 4NS, United Kingdom

Received: August 8, 2000

The conformational preferences of the diastereomeric neurotransmitters (1R2S) ephedrine and (1S2S) pseudoephedrine have been studied in the gas phase, under free jet-expansion conditions, using ultraviolet spectroscopy (both R2PI and LIF) and infrared ion-dip and hole-burning spectroscopy in combination with *ab initio* calculation. This has led to the identification and assignment of two conformers in ephedrine and four in pseudoephedrine. Assignments have been made by comparing their experimental infrared and LIF spectra with *ab initio* vibrational frequencies and ultraviolet rotational band contours. The relative stabilities of the conformers are controlled by a delicate balance between intramolecular hydrogen bonding and dispersive interactions between the methyl groups of the side chain, both with each other and with the aromatic ring. The relative conformational stabilities calculated for ephedrine do not agree with the experimental results; two of its low-lying conformers were detected, but a third, lying at an intermediate energy, was not. The possibility of its collisional relaxation into the global minimum during the supersonic expansion was not supported by the *ab initio* calculations, which predict a substantial barrier along the minimum energy pathway. It is possible that the combination of a relatively weak transition moment and a lack of facile pathways for relaxation from *higher* lying structures *into* the “missing” conformer may play a role.

1. Introduction

The internal biochemistry of the human body is regulated by a number of relatively small molecules known as neurotransmitters.^{1,2} Prominent examples include dopamine, which is ubiquitous in the brain and central nervous system, and adrenaline which acts to increase both heart rate and respiration. As might be expected, synthetic analogues of such molecules constitute a significant fraction of commercially available pharmaceuticals with numerous examples including the anti-asthma drug salbutamol, and propranolol, one of a series of drugs commonly known as beta-blockers. The design of such drugs has generally been optimized by systematically altering the functional groups of a known compound (such as adrenaline) and testing the resulting species for effectiveness, selectivity and toxicity. Rational drug design can be facilitated by a better understanding of the structures involved particularly with regard to the binding site of the receptor^{3,4} and by more complete studies of the conformational preferences of the neurotransmitter itself.

Toward this end, an exploration of the conformational landscapes of a number of natural and man-made neurotransmitters has been initiated, using a combination of gas-phase spectroscopy and *ab initio* calculation. The initial choice has comprised the diastereomeric pair (1R2S) ephedrine and (1S2S) pseudoephedrine; their structures are shown in Figure 1. These molecules, which differ only by the chirality of one center, are related to adrenaline and have similar effects on the

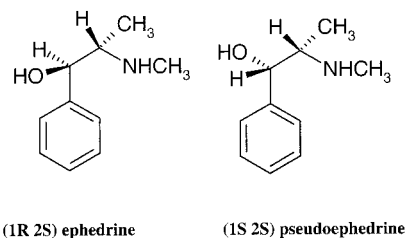


Figure 1. Structures of (1R2S) ephedrine and (1S2S) pseudoephedrine.

cardiovascular system. The receptors that such molecules target are embedded in the membrane wall of the cell and consist of a single protein strand.^{3,4} Binding of adrenaline and its analogues to these adrenoceptors results in a conformational change of the protein which releases further species into the cell. The binding site of the receptor is believed to contain amino acid residues (serine and aspartic acid) which can hydrogen bond to both the ethanolamine side chain and, in the catecholamine series, to the hydroxy groups of the catechol ring.⁴ Further interactions between the neurotransmitter and amino acids (including π - π interactions or dispersive interactions between alkyl groups) are also believed to play a role.

Ephedrine has been used in the treatment of asthma while pseudoephedrine is a common ingredient in cough medicine where it acts as a decongestant.¹ Such differing physiological effects highlight the importance of chirality in nature. This has been examined in the gas phase by several recent studies of clusters of chiral molecules.^{5–7} By making clusters between a racemic mixture of one molecule (R and S enantiomers) and a single enantiomer of another (for example the R enantiomer) the RR and SR diastereomers could be distinguished spectroscopically. The discrimination between such diastereomers was

* Corresponding author. Fax +44 1865 275410. E-mail: jpsimons@physchem.ox.ac.uk.

[†] University of Oxford.

[‡] University of London.

greatly facilitated by the differing strengths of the nonbonded interactions between the partners, including hydrogen bonding and dispersion forces between flexible side chains and aromatic rings. Similar effects should be expected for ephedrine and pseudoephedrine where the two chiral centers are incorporated in the same molecule. As an example of the striking differences that the change of a single chiral center can make, the melting point⁸ of ephedrine is 36 °C but that of pseudoephedrine is 120 °C.

Previous spectroscopic studies of the ephedra series of pharmaceuticals are limited. Freedman and co-workers⁹ have studied the vibrational circular dichroism of ephedrine, pseudoephedrine, and a number of related species in C₂Cl₄ solutions and were able to resolve OH vibrational bands that indicated the presence of both free and intramolecularly bound hydroxy groups. Low-level ab initio calculations using the 3-21G basis set indicated substantial differences in the conformational preferences of ephedrine and pseudoephedrine with the latter having four low-lying conformers compared with only two for ephedrine. The gas-phase infrared absorption spectrum of ephedrine¹⁰ shows three distinct OH stretching modes (two in the intramolecular hydrogen bound region and one in the free alcohol region).

Recent work on a related molecule, 2-amino-1-phenylethanol (referred to as APE), identified two conformers, one with an extended side chain and one folded. A combination of rotational band contour analysis, infrared spectroscopy and ab initio calculation¹¹ allowed their structural assignment. Both conformers were stabilized by an intramolecular hydrogen bond between the neighboring OH and NH₂ groups with the OH group acting as the proton donor. This result helped to inspire the present study of ephedrine and pseudoephedrine, where the introduction of a second chiral center, defines their chiralities as (1R2S) and (1S2S), respectively.

2. Methods

The systems used for mass selected resonant 2-photon ionization (R2PI) and laser-induced fluorescence (LIF) are identical to those described previously.^{11–13} A free jet expansion of ephedrine or pseudoephedrine was generated in a heated (ca. 110 °C) pulsed valve operated with a typical backing pressure of 3 bar of helium. (1R2S) ephedrine and (1S2S) pseudoephedrine were obtained from Fluka (purity >98%) and used without further purification.

IR/UV hole-burning spectra were obtained using two electronically synchronized YAG-pumped dye lasers. UV radiation was produced by the frequency-doubled output of a Lambda Physik dye laser (FL2002) pumped by the third harmonic of a Nd:YAG laser. Typical UV pulse energies, of the order of 500 μJ, were focused into the ionization region of a time-of-flight mass spectrometer (Jordan) with a 1 m focal length quartz lens. Tunable infrared radiation in the region of 2.8 μm was generated in a LiNbO₃ difference frequency module at the output of a YAG-pumped dye laser (Continuum Powerlite and ND6000). Typical IR pulse energies, ca. 2 mJ, were passed through the chamber antiparallel to the UV beam with a 25 cm focal length CaF₂ lens. The IR laser was fired approximately 100 ns before the UV laser to deplete the populations of the electronic ground state of the molecule. Two types of experiment were conducted. In one, the UV laser was tuned onto a selected R2PI feature, while the IR laser was scanned over the mid-IR range, from ca. 3800–3300 cm⁻¹ to record an IR ion-dip spectrum. In the other, the UV laser was scanned while the IR laser frequency was locked on to a particular IR absorption band to record an

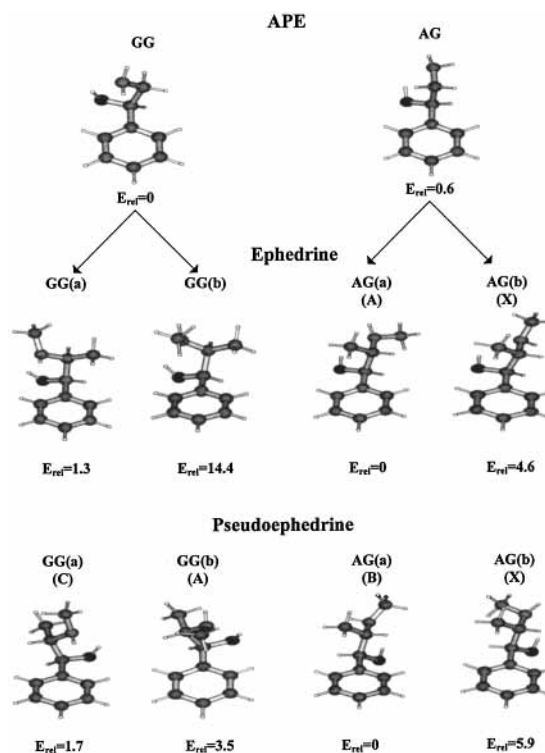


Figure 2. Ab initio structures of the lowest lying conformers of APE, ephedrine and pseudoephedrine. Energies are calculated at the HF/6-31G* optimized geometries by single-point MP2/6-31G*. Relative energies are given in kJ mol⁻¹ and include zero-point corrections. Assignments to individual peaks in the R2PI spectra (see later) are also shown.

IR hole-burn R2PI spectrum. In this way it was possible to separate all the conformers present in the expansion and record their IR absorption spectra independently.

LIF spectra were also recorded, initially at low resolution (0.3 cm⁻¹) using the frequency-doubled output of an excimer (Lambda Physik EMG201, XeCl fill) pumped dye laser (Lambda Physik FL3002). Partially resolved rotational band contours were then obtained by the introduction of an intracavity etalon which reduced the bandwidth of the UV laser pulse to approximately 0.09 cm⁻¹; these were simulated using methods described elsewhere.¹⁴

Ab initio calculations were performed using the Gaussian suite of programs.¹⁵ Initial structures of ephedrine and pseudoephedrine were based on those calculated for the seven most stable conformers of APE.¹¹ Geometries were optimized at the HF/6-31G* level after which single-point calculations were performed using the MP2 level of theory with the same, or more extended basis sets to determine their relative energies. Excited-state rotational constants and transition dipole moments were calculated using the CIS method with a 6-31G* basis set. Vibrational frequencies were calculated using the B3LYP density functional method with a 6-31+G* basis set which has been found to yield fair agreement with experimental data for similar molecules^{11–13,16} when scaling factors of 0.9734 for OH stretching modes and 0.956 for NH are used. These factors are derived from previous work on APE¹¹ and phenylalanine.¹⁶

3. Results

3.1. Ab Initio Calculations. The most stable conformational structures of ephedrine and pseudoephedrine, calculated at the HF/6-31G* level of theory, are presented in Figure 2, together with those of APE¹¹ shown for comparison. The ab initio

TABLE 1: Calculated Constants for All Four Low-Lying Conformers (GG(a), GG(b), AG(a) and AG(b)) of Ephedrine^a

	GG(a)	GG(b)	AG(a)	AG(b)
$\Delta E/\text{kJ mol}^{-1}$	1.3	14.4	0.0	4.6
$\Delta G_{\text{rel}}/\text{kJ mol}^{-1}$	4.3	19.4	0.0	5.8
$\angle \text{OCCN}/\text{deg}$	56	52	57	60
$\text{OH}\cdots\text{N}/\text{pm}$	220	217	225	226
$\angle \text{OHN}/\text{deg}$	117	118	114	114
A''/MHz	1596.8	1456.9	1990.5	2167.0
B''/MHz	586.4	651.1	527.2	498.4
C''/MHz	561.2	633.1	493.2	471.0
A'/MHz	1579.3	1443.3	1963.1	2121.2
B'/MHz	579.4	646.4	524.2	496.2
C'/MHz	555.6	625.2	490.0	468.1
$\mu_a^2:\mu_b^2:\mu_c^2$	22:77:1	46:51:3	62:34:4	73:26:1
$ \mu_{\text{trans}} \times 10^{30}/\text{C m}$	0.63	1.04	1.13	1.10

^a Ground state structural parameters and rotational constants are from HF/6-31G* optimized geometries. Excited state rotational constants and transition dipole moments are from CIS/6-31G* calculations. The relative energies (single point MP2/6-31G* at the HF/6-31G* optimized geometries) of the conformers include zero-point corrections.

TABLE 2: Calculated Constants for All Four Low-Lying Conformers (GG(a), GG(b), AG(a), and AG(b)) of Pseudoephedrine^a

	GG(a)	GG(b)	AG(a)	AG(b)
$\Delta E/\text{kJ mol}^{-1}$	1.7	3.5	0.0	5.9
$\angle \text{OCCN}/\text{deg}$	57	50	51	49
$\text{OH}\cdots\text{N}/\text{pm}$	222	216	214	212
$\angle \text{OHN}/\text{deg}$	115	117	117	119
A''/MHz	1690.5	1637.8	2059.6	2095.5
B''/MHz	553.9	595.5	506.5	524.8
C''/MHz	533.0	576.7	472.5	481.6
A'/MHz	1658.2	1623.1	2010.5	2053.4
B'/MHz	547.7	588.8	504.9	523.1
C'/MHz	531.2	576.0	469.2	477.6
$\mu_a^2:\mu_b^2:\mu_c^2$	63:17:20	57:7:36	22:72:6	14:78:8
$ \mu_{\text{trans}} \times 10^{30}/\text{C m}$	1.20	1.39	0.35	0.37

^a Ground state structural parameters and rotational constants are from HF/6-31G* optimized geometries. Excited state rotational constants and transition dipole moments are from CIS/6-31G* calculations. The relative energies (single point MP2/6-31G* at the HF/6-31G* optimized geometries) of the conformers include zero-point corrections.

structural data for each of the low-lying conformers are shown in Tables 1 and 2 for ephedrine and pseudoephedrine, respectively. The A/G notation refers to the arrangement (anti or gauche) of the CCCN and OCCN atom chains, respectively. The introduction of an *N*-methyl group in ephedrine and pseudoephedrine doubles the number of possible conformers. If the barriers to inversion of the amino group are sufficiently high, the two configurations will be locked into place in the cold environment of the supersonic expansion: they have been labeled (a) and (b) in Figure 2.

In each case the extended, AG, and folded, GG, conformational structures lie very close in energy, with AG(a) predicted to be the most stable structure in both ephedrine and pseudoephedrine. In APE, where the predicted ordering is "too close to call", experimental measurements have also established a mild preference for the extended AG conformational structure (though the situation is reversed in its 1:1 hydrated complex¹¹). The alternative conformers, labeled AG(b), GG(a), and GG(b), are located at slightly higher energies in pseudoephedrine but, in its diastereoisomer ephedrine, the folded GG(b) conformer is much less stable. As in APE,¹¹ all four conformers enjoy the benefit of an intramolecular hydrogen bond directed from the OH group toward the neighboring (methyl) amino group. Conformers in which the direction of the hydrogen bond is

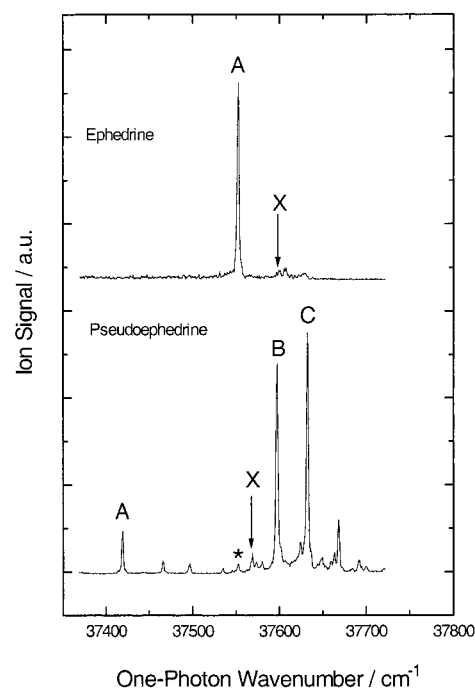


Figure 3. Resonant two-photon ionization (R2PI) spectra of ephedrine and pseudoephedrine. Both spectra were recorded on the $m/z = 58$ mass channel corresponding to the side-chain fragment ion ($\text{CH}(\text{CH}_3)\text{-NHCH}_3^+$). The feature marked with an asterisk in the pseudoephedrine spectrum is due to an ephedrine impurity.

reversed, with amino the donor and OH the accepting group, lie at much higher energies. In summary, the ab initio calculations suggest somewhat different conformational landscapes in the two diastereoisomers with four low-lying structures anticipated in pseudoephedrine and three in ephedrine. In both cases the most stable conformer has the extended AG(a) structure.

3.2. UV Spectroscopy of Ephedrine and Pseudoephedrine.

Mass-selected R2PI spectra of ephedrine and pseudoephedrine are shown in Figure 3. The molecular ions of both species undergo efficient fragmentation with the side-chain fragment containing the (methyl) amino group ($\text{CH}(\text{CH}_3)\text{NHCH}_3$, $m/z = 58$) the most abundant. Similar ion fragmentation was observed by Bernstein and co-workers in the R2PI spectrum of amphetamine¹⁷ and by Robertson and co-workers in 2-phenylethylamine.¹⁸ The addition of a methyl to the amino group results in further stabilization of the side-chain ion and a higher degree of fragmentation. The spectra of the two diastereoisomers are strikingly different. Ephedrine shows only one intense band, feature A (37553 cm^{-1}), with some weak structure to the blue but pseudoephedrine displays three intense bands, A (37420 cm^{-1}), B (37598 cm^{-1}), and C (37633 cm^{-1}) with many other weaker features spread over a range of several hundred wavenumbers. The features marked X for both molecules (37598 cm^{-1} for ephedrine and 37569 cm^{-1} for pseudoephedrine) are distinct conformers whose identification will be discussed in the next section. Feature X in ephedrine occurs at the same wavenumber as band B of pseudoephedrine. However, since no sign of a band at the energy of band C can be observed in the ephedrine spectrum, we assume that feature X of ephedrine is a distinct conformer (this assumption is shown to be correct by infrared spectroscopy (see later)).

Partially resolved rotational band contours of features A and X of ephedrine and features A, B, and C of pseudoephedrine are shown in Figures 4 and 5 alongside those calculated¹⁴ for each of the four low-lying conformers of both molecules. Comparison of these contours, taking into account calculated

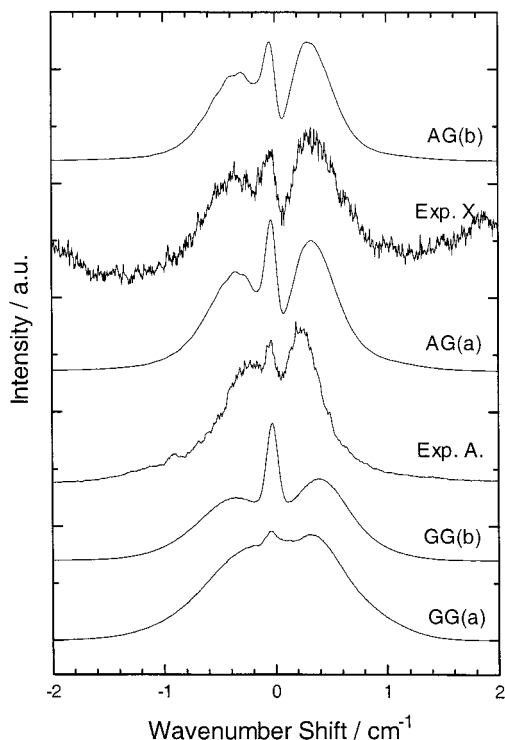


Figure 4. Partially resolved rotational band contour of ephedrine (features A and X) obtained by laser-induced fluorescence. Also shown are the calculated contours for the four low-lying conformers (GG(a), GG(b), AG(a), and AG(b)) using a laser line width of 0.1 cm^{-1} and a rotational temperature of 3.5 K. Ground-state rotational constants from HF/6-31G* calculations while excited-state constants and transition dipole moments are from CIS/6-31G*.

relative energies shown in Figure 2, allows assignment of feature A in ephedrine and feature B in pseudoephedrine to the band origins of the conformational structure, AG(a). Feature X in ephedrine is assigned to the less stable extended conformer, AG(b), and features A and C of pseudoephedrine are tentatively assigned to the band origins of conformers GG(b) and GG(a), respectively; their band contours are too similar to allow a more confident assignment at this stage (but see the next section). Tables 1 and 2 list the rotational constants and $S_1 \leftarrow S_0$ hybrid values for the low-lying conformers of ephedrine and pseudoephedrine.

3.3. IR Spectroscopy of Ephedrine and Pseudoephedrine.

(a) Ephedrine. The infrared ion-dip and R2PI hole-burn spectra of ephedrine are shown in Figures 6 and 7. In the hole-burn spectra, where the UV laser is scanned while the IR “burn” laser is tuned on to peak A, the R2PI signal associated with A is strongly depleted but the small peak X, identified in Figure 3, remains unaffected. It is assigned, therefore, to a second distinct conformer. The infrared ion-dip spectra associated with conformers A and X both display an intense feature, lying at 3493 and 3540 cm^{-1} , respectively, and assigned to the O–H stretching vibration. Its red shift relative to the O–H stretch frequency in ethanol (lying ca. $3650\text{--}3680 \text{ cm}^{-1}$)¹⁹ is typical of that introduced by an intramolecular H-bond in which the OH group acts as the proton donor to a neighboring amino group.¹¹ The weaker feature associated with conformer A, lying at 3378 cm^{-1} , is assigned to the N–H stretching mode; its frequency can be compared with that of the corresponding band in dimethylamine,¹⁰ which lies at 3375 cm^{-1} . For band X no sign of the NH stretch is observed. To the blue of the OH band a weak doublet feature is observed (3542 and 3552 cm^{-1}). Similar features are observed for pseudoephedrine (see next

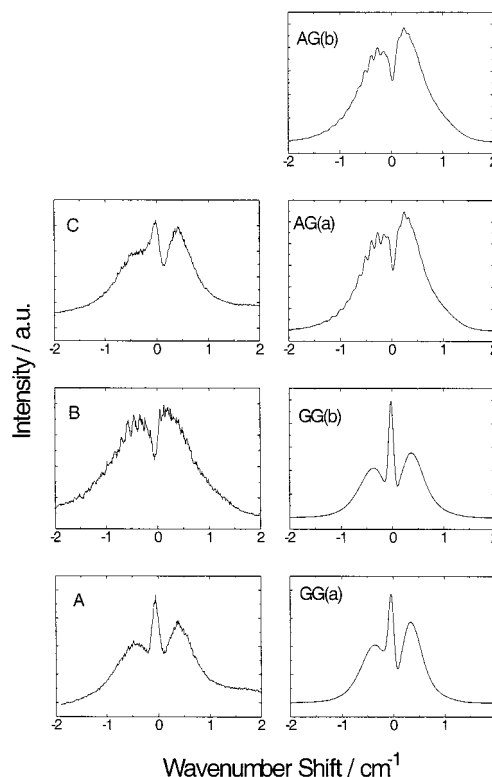


Figure 5. Partially resolved rotational band contours of pseudoephedrine (features A, B, and C) obtained by laser-induced fluorescence. Also shown are the calculated contours for the four low-lying conformers (GG(a), GG(b), AG(a), and AG(b)) using a laser line width of 0.1 cm^{-1} and a rotational temperature of 3.5 K. Ground-state rotational constants from HF/6-31G* calculations while excited-state constants and transition dipole moments are from CIS/6-31G*.

section) and for the related molecules norephedrine and α -(methyaminomethyl) benzyl alcohol.²⁰ We tentatively assign these to combination bands of the OH stretching mode with a low-frequency mode of the molecule.

The O–H and N–H frequencies calculated ab initio, for each of the three lowest lying conformers, AG(a), GG(a) and AG(b) of ephedrine, are listed in Table 3 and are also shown in Figure 6. The agreement between the O–H and N–H frequencies recorded for conformer A and those calculated for the structure AG(a), is excellent, establishing its assignment. The assignment of conformer X is less straightforward. Excellent agreement between the observed and calculated O–H frequencies is found, not for the expected structure GG(a), anticipated on the basis of its calculated relative energy (see Figure 2), but for the higher energy conformational structure, AG(b). Calculations conducted at higher levels of theory, using larger basis sets and including electron correlation (see Table 4), did not alter the predicted energy ordering. The apparent absence of the folded GG(a) conformation in the jet-cooled expansion will be discussed further in section 4.2.

(b) Pseudoephedrine. The infrared ion-dip and R2PI hole-burn spectra of pseudoephedrine are shown in Figures 8 and 9. The peaks labeled A, B, and C can be identified as the band origins of three distinct conformers and the hole-burn spectrum based on the weak feature labeled X, in Figure 3, reveals a fourth. The hole-burn spectrum based upon peak A also reveals its association with a weak, low-frequency vibrational progression running toward higher frequencies. As with ephedrine, the infrared ion-dip spectra shown in Figure 8 are dominated by the O–H stretching modes, which again lie in the spectral region expected for an intramolecular H-bonded interaction, 3437 cm^{-1}

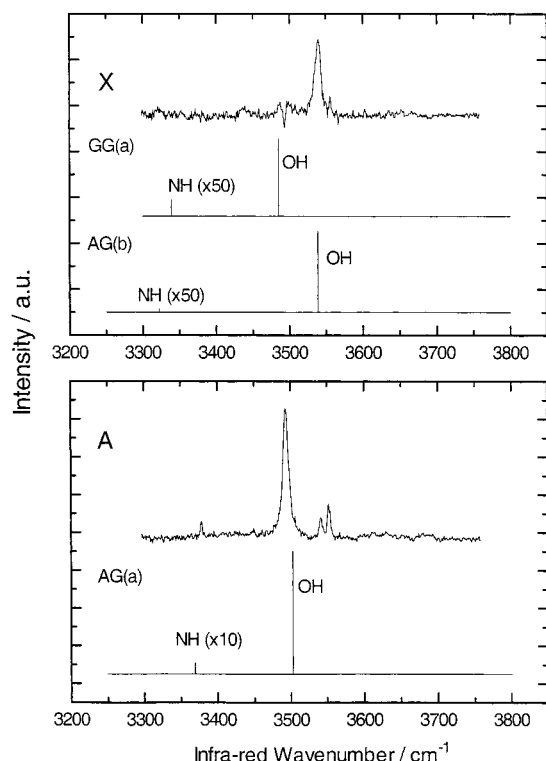


Figure 6. Infrared ion-dip spectra of features A and X of ephedrine. Also shown are calculated stick spectra for the three lowest lying conformers (GG(a), AG(a), and AG(b)). Calculations were performed using the B3LYP method with a 6-31+G* basis set. OH and NH frequencies have been scaled by factors of 0.9734 and 0.956, respectively, derived from previous work on APE¹¹ and phenylalanine.¹⁶

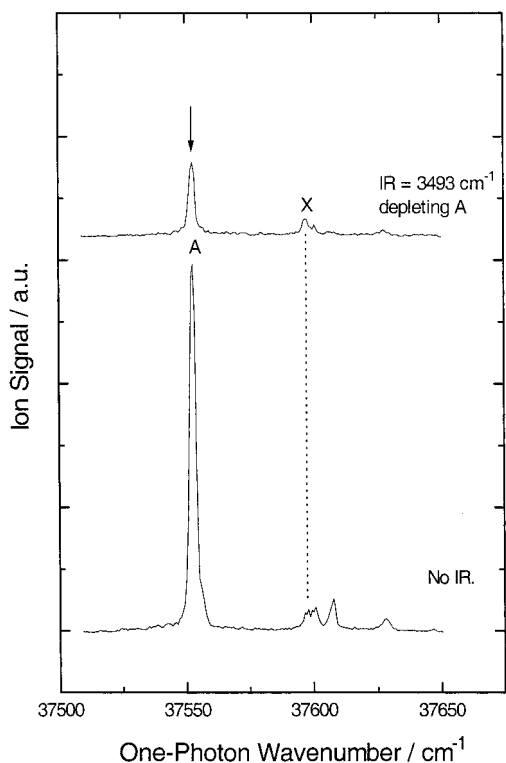


Figure 7. Resonant two-photon ionization (R2PI) hole-burn spectra of ephedrine. The lower trace shows the spectrum recorded with no infrared present while the upper panel shows the same for the IR frequency tuned to deplete feature A (3493 cm⁻¹).

(A), 3477 cm⁻¹ (B), 3515 cm⁻¹ (C), and 3454 cm⁻¹ (X). The O–H and N–H vibrational frequencies, calculated ab initio,

TABLE 3: Experimental and Calculated Vibrational Frequencies of Ephedrine^a

	A	AG(a)	X	AG(b)	GG(a)
OH stretch/cm ⁻¹	3493	3503 (111)	3540	3539 (104)	3485 (118)
NH stretch/cm ⁻¹	3378	3369 (1)	—	3322 (0.1)	3339 (0.5)

^a The calculated OH and NH frequencies have been scaled by factors of 0.9734 and 0.956, respectively (derived from previous work on APE¹¹ and phenylalanine¹⁶). Numbers in parentheses are the calculated relative intensities of the vibrational modes.

for each of the four low-lying conformational structures of pseudoephedrine, are compared with those recorded experimentally in Table 5, and are also presented in Figure 8. The excellent agreement between the experimental and calculated frequencies confirms the assignment of conformer B to the structure AG(a) (predicted to be the most stable, although band C in the R2PI spectrum is slightly more intense) and allows the unambiguous assignment of conformers A and C, to the two folded structures GG(b) and GG(a), respectively. This confirms the tentative assignments that were based upon the rotational band contour simulations shown in Figure 5. Conformer X can be assigned to the structure AG(b).

The considerable red shift (50 cm⁻¹) in the relatively intense N–H band, in changing from conformer A to conformer C, can be ascribed to the change in the orientation of the terminal methyl amino group (see Figure 2). The GG(a) structure of conformer C, which directs the N–H bond toward the ring, allows an NH... π -aromatic H-bonded interaction and the consequent red shift. Conversely, the large red-shift in the O–H frequency, $\delta\nu = 78$ cm⁻¹, which follows the change from conformer C to conformer A, is also striking, particularly since the O–H frequency in conformer C is virtually identical to that in the corresponding folded, H-bonded GG structure, in the non-methylated analogue, APE.¹¹ The GG(b) conformation of A must allow a rather stronger H-bonded interaction with the methylamino group than it does in the alternative GG(a) structure, conformer C (see discussion section 4.1). The resulting frequency shifts have another consequence—they bring the N–H and O–H modes in conformer A (GG(b)) into near-degeneracy. This is particularly clear in the ab initio calculation on conformer A which predicts near equal (harmonic) frequencies for the two modes with strong coupling between them resulting in substantial intensity in *each* of the two transitions. Such coupling is not observed experimentally, however; because of this the O–H and N–H frequencies were recalculated using the partially deuterated molecules, NH/OD and ND/OH. In the event, the frequencies did not change but the relative intensity of the NH band fell by approximately 2 orders of magnitude (see Figure 8).

4. Discussion

4.1. Conformational Preferences. The conformational preferences of ephedrine and pseudoephedrine are controlled by a delicate balance of competing factors; as with the APE molecule,¹¹ the most important is the intramolecular hydrogen bond between the hydroxyl and (methyl) amino groups. The most stable conformers are those in which the hydroxyl group acts as proton donor. The bonds are strained (typical OHN angles of 115°–120°) and are slightly longer than found for the phenol-ammonia cluster²¹ (OH \rightarrow N bond lengths of 210–230 pm versus 199 pm) because of the constraints introduced by the geometry of the side chain. Superimposed onto this effect are the interactions of the two methyl groups with each other

TABLE 4: Relative Energies for the Four Low-lying Conformers of Ephedrine Calculated at Different Levels of Theory^a

conformer	single-point MP2/6-31G**// HF/6-31G* (kJ mol ⁻¹)	MP2/6-31+G* (kJ mol ⁻¹)	MP2/6-311G** (kJ mol ⁻¹)	single-point MP2/6-311+G**// B3LYP/6-31+G* (kJ mol ⁻¹)
GG(a)	1.3	3.1	2.5	3.1
GG(b)	14.4	15.6	13.1	15.0
AG(a)	0	0	0	0
AG(b)	4.6	5.8	5.3	5.2

^a MP2/6-31G**//HF/6-31G* indicates single-point MP2 calculations at the HF/6-31G* optimized geometry. MP2/6-311+G**//B3LYP/6-31+G* indicates single-point MP2/6-311+G** calculations at the geometries optimized at the B3LYP/6-31+G* level. Zero-point corrections are included with a scaling factor of 0.976.

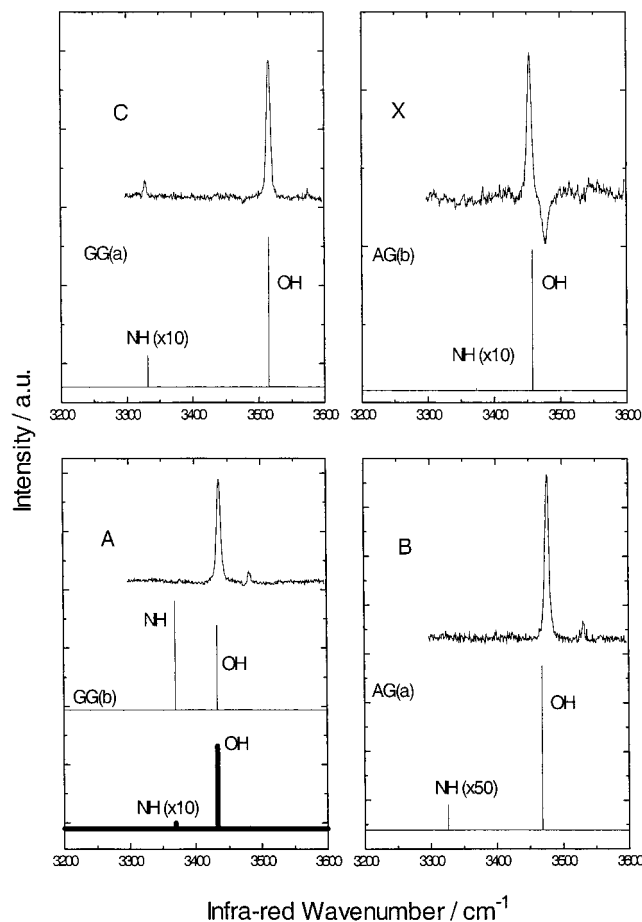


Figure 8. Infrared ion-dip spectra of features A, B, C, and X of pseudoephedrine. Also shown are calculated stick spectra for the four lowest lying conformers (GG(a), GG(b), AG(a), and AG(b)). Calculations were performed using the B3LYP method with a 6-31+G* basis set. OH and NH frequencies have been scaled by factors of 0.9734 and 0.956, respectively, derived from previous work on APE¹¹ and phenylalanine.¹⁶ For conformer GG(b) the unscaled vibrational frequencies of the OH and NH stretching modes are almost degenerate resulting in substantial interaction and intensity borrowing. To compensate for this effect, which is not observed experimentally, calculations of the partially deuterated molecule (i.e., NH/OD and ND/OH) were performed to obtain unperturbed frequencies and intensities for the OH and NH stretching modes. These are shown as bold lines on the plot.

(in a fashion similar to that of butane²²) and with the aromatic ring. A weak hydrogen bond between the NH group and the π -system of the ring can introduce a further interaction. This interaction (which exists for conformer GG(a) of both ephedrine and pseudoephedrine) has already been found to have an important effect on the conformational landscapes of several molecules including phenylethylamine,¹⁸ amphetamine,¹⁷ and phenylalanine.¹⁶ When taken together, such interactions affect both the relative energies of the conformers and, through

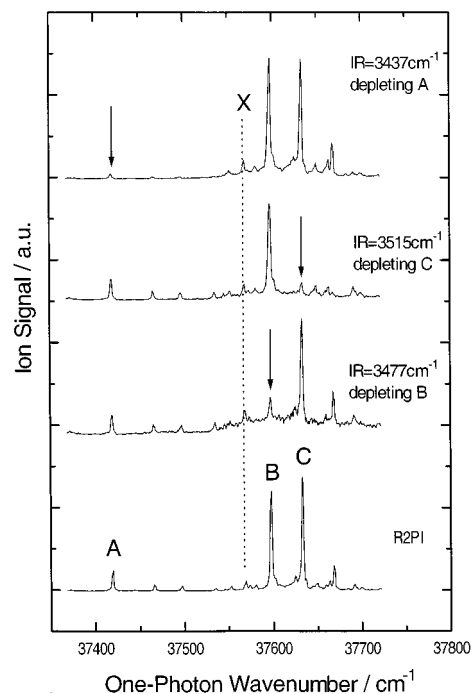


Figure 9. Resonant two-photon ionization (R2PI) hole-burn spectra of pseudoephedrine. The lower trace shows the spectrum recorded with no infrared present while the three upper traces show the same for the IR frequency tuned to deplete features A (3437 cm⁻¹), B (3477 cm⁻¹), and C (3515 cm⁻¹), respectively.

cooperative effects, the strength of the primary hydrogen-bonded interaction between the neighboring hydroxyl and amino groups.

The conformer structure GG(b) provides an excellent example of these interactions. In ephedrine the conformer lies at high energy (ca. 14 kJ mol⁻¹) and is not observed experimentally. However, the change of one chiral center, in pseudoephedrine, results in the conformer lying at relatively low energy (3.5 kJ mol⁻¹) where it can be assigned to peak A. Both diastereoisomers are destabilized (relative to the structure GG(a)) by the interaction of the *N*-methyl group with the aromatic ring and by the loss of the NH to π bond. Furthermore, in the GG(b) structure of ephedrine the two methyl groups adopt a conformation which is almost eclipsed resulting in the further destabilization of the conformer. On the other hand, the analogous structure in pseudoephedrine has the methyl groups arranged in a fashion which is very close to that of the staggered (and most energetically favorable) conformation of butane.²² It is also interesting to note that feature A (conformer GG(b)) in pseudoephedrine is considerably red-shifted in the UV spectrum (by ca. 200 cm⁻¹) relative to peak C (conformer GG(a)). Such a shift is an indication of the interaction in conformer GG(b) of the *N*-methyl group with the π -system of the aromatic ring. Such discrimination between very similar conformers is in line with the separation of diastereomeric clusters.⁵⁻⁷

TABLE 5: Experimental and Calculated Vibrational Frequencies of Pseudoephedrine^a

	A	GG(b)	B	AG(a)	C	GG(a)	X	AG(b)
OH stretch/cm ⁻¹	3437	3433 (142)	3477	3469(162)	3515	3515 (96)	3454	3458(170)
NH stretch/cm ⁻¹	3378	3526 (1)	—	3326 (0.5)	3328	3332 (2)	3383	3373 (2)

^a The OH and NH frequencies have been scaled by factors of 0.9734 and 0.956, respectively (derived from previous work on APE¹¹ and phenylalanine¹⁶). The ab initio frequencies for conformer GG(b) were determined from isotopically substituted NH and OH groups to avoid the mode mixing mentioned in the text. Numbers in parentheses are the calculated relative intensities of the vibrational modes.

The conformer structures GG(a) and GG(b) in pseudoephedrine also manifest the effects of such interactions in their infrared absorption spectra with GG(b) having an O–H vibrational frequency that is red-shifted by 78 cm⁻¹ relative to that of GG(a). The distortion of the side chain in GG(b) (OCCN dihedral angle of 50° at the HF/6-31G* level relative to a dihedral angle of 57° in GG(a)) caused by the interaction of the *N*-methyl group with the aromatic ring results in a sizable shortening of the hydrogen bond (216 pm versus 222 pm) and a slightly more favorable angle (∠OHN = 117° versus 115°) for intramolecular hydrogen bonding.

4.2. Conformer Relaxation. The combination of ab initio calculations with rotational band contour analysis and infrared spectroscopy has enabled the structural assignment of each of the observed conformers. However, the discrepancy between the conformer populations predicted ab initio and the experimental observations in the case of ephedrine requires some comment. The relative energy calculations suggest that three conformers of ephedrine might be expected to appear in its R2PI spectrum. Assuming a Boltzmann population distribution at the stagnation temperature behind the pulsed valve, the missing conformer (GG(a)) should be observed with an intensity intermediate between that of features A and X. The fact that it is not observed has wider implications for the assignment of conformers in similar experiments. Simply assuming that the relative intensities of features in a R2PI or LIF spectrum can be directly linked to the calculated relative energies of each conformer may result in misassignments.^{24,25} Following such a path the natural assumption would be that features A and X of ephedrine would be assigned to conformers AG(a) and GG(a), respectively. For pseudoephedrine the assignments would be A, GG(b); B, GG(a); C, AG(a); and X, AG(b). Such assignments (particularly feature X of ephedrine and features A and C of pseudoephedrine) are not confirmed by their observed vibrational spectra or rotational band contours and one or more of the assumptions implicit in these assignments must be invalid.

To recapitulate, the assumptions are as follows: first, that the relative energy ordering predicted by the ab initio calculations is reliable; second that the S₁ ← S₀ transition dipole strengths are insensitive to changes in the side-chain conformation; third, that the S₁ ← S₀ transition associated with the “missing conformer” of ephedrine lies inside the spectral region scanned in the R2PI spectrum; and fourth, that the relative conformer populations established in the environment of the cold, free-jet gas expansion correspond to those maintained at thermal equilibrium at the initial, preexpansion, stagnation temperature and finally that the entropies of each conformer are similar enough that the relative energy, $\Delta E \approx \Delta G$, the relative free energy. The first assumption is unlikely to present a problem since the calculated relative conformer stabilities were unchanged by increasing refinements in the level of theory used (see Table 4). Similarly, the calculated transition dipole strengths of each of the ephedrine conformers, listed in Table 1, are all of comparable magnitude (although the transition moment alignments are sensitive to conformational change). The third assumption is also unlikely to be wrong since the R2PI spectra of both molecules were scanned over a wide frequency range:

in addition, the analogue of the “missing GG(a) ephedrine conformer” is observed in the R2PI spectrum of norephedrine (ephedrine without the *N*-methyl group),²⁰ despite its increased relative energy, predicted by the ab initio calculations (compare the data listed in Tables 1 and 2). Its band origin is displaced to the blue of the corresponding band in the AG(a) conformer,²⁰ by ca. 50 cm⁻¹ (a similar shift is also observed between peaks B and C of pseudoephedrine in Figure 3). Suspicion falls therefore on the final assumptions, which tacitly ignore the possibility of conformational relaxation^{23–25} during the expansion period and possible changes in the frequencies and anharmonicities of low-lying vibrational modes, e.g., hindered methyl rotations. The latter assumption was examined by calculating the relative free energies (ΔG) of each of the low-lying conformers, assuming all the contributing vibrational modes were harmonic. The relative energies, shown in Table 1 for the four lowest-lying conformers of ephedrine, showed no change in the overall energy ordering of the conformers although the energy separation between GG(a) and AG(a) does increase somewhat when the calculated entropy change is included. In combination with the smaller transition moment of structure GG(a) this might help to explain why this conformer could not be observed experimentally.

The rates/relative probabilities of conformational relaxation depend on the height(s) of the potential energy barrier(s) which separate neighboring conformational minima. If the barriers are sufficiently low,²³ typically \leq ca. 500 cm⁻¹, the interconversion rates are likely to be fast enough to allow significant relaxation.^{24,25} Some of the predicted low-lying conformers of alanine and glycine, for example, which were expected to appear in their microwave spectra recorded under free-jet expansion conditions, could not be detected; their absence correlated with the predicted availability of low energy barrier (<500 cm⁻¹) pathways for their relaxation.^{24,25}

On the other hand, the minimum barrier heights calculated for relaxation of conformer GG(a) to AG(a) in ephedrine (1055 cm⁻¹ (B3LYP/6-31+G*) and 1400 cm⁻¹ (MP2/6-31+G*)) are such that facile relaxation would *not* be expected to occur during the expansion. (The barrier corresponds to the first-order transition state accessed via a clockwise torsion of the side chain about the C_{arom}–C_α–C_β–N dihedral angle, with all remaining degrees of freedom left free.) Attempts to find a lower energy pathway proved unsuccessful. Hence relaxation from GG(a) to AG(a) cannot account for the absence of GG(a) from the experimental spectra. We can, however, speculate on relaxation from *higher* conformational states. That such conformers exist at the temperature of the source is indicated by the presence of free OH stretching modes in the gas-phase IR absorption spectra.¹⁰ On the other hand, they were not detected in the jet-cooled ephedrines. Collisional relaxation of such conformers (as well as those that are endowed with an intramolecular hydrogen bond) into the low(er)-lying structures during the free-jet expansion, would result in non-Boltzmann population distributions,^{23–25} and lead to a relative increase in the population of the lower-lying conformers, A (AG(a)) and X (AG(b)). The absence of conformer GG(a) might then be attributed to a lack of energetically favorable pathways, allowing its population

via relaxation from the weakly populated *higher* energy conformations.

4.3. Relevance to Biological Processes. The markedly different conformational landscapes in the diastereoisomers, ephedrine and pseudoephedrine, reflect the influence of local molecular geometry changes on the balance of nonbonded interactions within the two molecules. These, in their turn, influence the structure and flexibility of their ethanolamine side chains, at least in the gas phase. In the condensed phase, dispersive, and particularly H-bonded interactions with the solvent might also be expected to have a substantial effect on the conformational landscape. Indeed, when the protic solvent molecule, water, is bound to an ethanolamine, as in the 1:1 complex with APE, the preferred conformation of the side chain switches from the extended AG structure to the folded GG structure.¹¹ Recent studies of multiply hydrated clusters of the peptide analogue, *N*-benzylformamide,²⁶ also reveal its conformational sensitivity to H-bonded and electrostatic interactions with the bound solvent molecules. The more flexible the side chain, the greater its conformational sensitivity to interactions with its neighbors. This may be crucial in a real biological system where "solvent" molecules (water) may bind to the neurotransmitter, which itself, may be bound as a ligand at (a) protein receptor site(s). Computer models⁴ appear to suggest that the binding site of adrenoceptors requires the ligand to have an extended side chain, with the amino group as far from the ring as possible. This is the preferred conformation in both "free" ephedrine and pseudoephedrine, but it remains to be seen whether this is maintained when they are bound to water molecules and/or to model adrenoceptor binding sites. Under physiological conditions, there are notable differences in the scale of response, when the two diastereoisomers are bound to adrenoceptor sites.²⁷ This is not too surprising in view of the chirality of both the receptor sites and the ligands, but their differing conformational landscapes (and side chain flexibility) revealed through the gas-phase experiments, may also contribute to their different physiological behavior.

5. Conclusions

A combination of R2PI spectroscopy, infrared hole-burn and ion-dip spectroscopy, and ab initio calculation has led to the identification and structural assignment of two conformers in ephedrine and four in pseudoephedrine. Each one is stabilized by intramolecular hydrogen bonding between the neighboring hydroxyl and methylamino groups, with the OH group acting as the proton donor, and both molecules adopt an extended side-chain conformation (AG(a)) at their global minima. The accessible conformational structures of the flexible ethanolamine side chain and the strength of the intramolecular hydrogen bonding along the chain are both dependent upon the delicate balance of steric and nonbonded interactions, involving the methyl groups on the side chain with each other, and with the aromatic ring, and also involving the weak H-bonded interaction between the (CH₃)NH group and the π -electrons on the aromatic ring. For ephedrine, a discrepancy exists in that the folded conformer (GG(a)), which at all levels of theory is expected to be low-lying, is not observed experimentally. The reasons for

this absence are not clear although a relatively weak transition moment and the lack of a facile relaxation pathway for higher lying conformers to the low-lying structure may play a role.

Acknowledgment. We are grateful for the financial support provided by EPSRC (N.A.M., P.B.), GlaxoWellcome (P.B.) and the Leverhulme Trust and for many helpful discussions with Dr. Evan Robertson and Professor George Tranter.

References and Notes

- (1) Snyder, S. H. *Drugs and the Brain*; Scientific American Library: New York, 1999.
- (2) Jeffrey, G. A.; Saenger, W. *Hydrogen Bonding in Biological Structures*; Springer-Verlag: Berlin, 1991.
- (3) Zigmond, M. J. *Fundamental Neuroscience*; Academic Press: London, 1998.
- (4) Strosberg, A. D. *Annu. Rev. Pharmacol. Toxicol.* **1997**, *37*, 421.
- (5) Al Rabaa, A.; Le Barbu, K.; Lahmani, F.; Zehnacker-Rentien, A. *J. Phys. Chem. A* **1997**, *101*, 3273.
- (6) Le Barbu, K.; Brenner, V.; Millie, P.; Lahmani, F.; Zehnacker-Rentien, A. *J. Phys. Chem. A* **1998**, *102*, 128.
- (7) Lahmani, F.; Le Barbu, K.; Zehnacker-Rentien, A. *J. Phys. Chem. A* **1999**, *103*, 1991.
- (8) Fluka Chemicals Catalogue, 1999/2000.
- (9) Freedman, T. B.; Ragunathan, N.; Alexander, S. *Faraday Discuss.* **1994**, *99*, 131.
- (10) NIST Mass Spectroscopy Data Center. Stein, S. E., Director. Infrared and Mass Spectra. In NIST chemistry Webbook: *NIST standard reference database*; Mallard, W. G., Linstrom, P. J., Eds.; National Institute of Standards and Technology: Gaithersburg, MD 20899 (<http://webbook.nist.gov>); February 2000, No. 69.
- (11) Graham, R. J.; Kroemer, R. T.; Mons, M.; Robertson, E. G.; Snoek, L. C.; Simons, J. P. *J. Phys. Chem. A* **1999**, *103*, 9706.
- (12) Mons, M.; Robertson, E. G.; Simons, J. P. *J. Phys. Chem. A* **2000**, *104*, 1430.
- (13) Robertson, E. G. *Chem. Phys. Lett.* **2000**, *104*, 299.
- (14) Hockridge, M. R.; Knight, S. M.; Robertson, E. G.; Simons, J. P.; McCombie, J.; Walker, M. *PCCP* **1999**, *1*, 407.
- (15) Frisch, M. J.; Trucks, G. W.; Schlegel, H. B.; Gill, P. M. W.; Johnson, B. G.; Robb, M. A.; Cheeseman, J. R.; Keith, T.; Petersson, G. A.; Montgomery, J. A.; Raghavachari, K.; Al-Laham, M. A.; Zakrzewski, V. G.; Ortiz, J. V.; Foresman, B.; Cioslowski, J.; Stefanov, B. B.; Nanayakkara, A.; Challacombe, M.; Peng, C. Y.; Ayala, P. Y.; Chen, W.; Wong, M. W.; Andres, J. L.; Replogle, E. S.; Gomperts, R.; Martin, R. L.; Fox, D. J.; Binkley, J. S.; Defrees, D. J.; Baker, J.; Stewart, J. P.; Head-Gordon, M.; Gonzalez, C.; Pople, J. A. *Gaussian 94*; revision C.3; Gaussian, Inc.: Pittsburgh, PA, 1995.
- (16) Snoek, L. C.; Robertson, E. G.; Kroemer, R. T.; Simons, J. P. *Chem. Phys. Lett.* **2000**, *321*, 49.
- (17) Yao, J.; Im, H. S.; Foltin, M.; Bernstein, E. R. *J. Phys. Chem. A* **2000**, *104*, 6117.
- (18) Dickinson, J. A.; Hockridge, M. R.; Kroemer, R. T.; Robertson, E. G.; Simons, J. P.; McCombie, J.; Walker, M. *J. Am. Chem. Soc.* **1998**, *120*, 2622.
- (19) Provencal, R. A.; Casaes, R. N.; Roth, K.; Paul, J. B.; Chappo, C. N.; Saykally, R. J.; Tschumper, G. S.; Schaefer, H. F., III. *J. Phys. Chem. A* **2000**, *104*, 1423.
- (20) Butz, P.; Kroemer, R. T.; Macleod, N. A.; Robertson, E. G.; Simons, J. P. *J. Phys. Chem. A*, submitted for publication.
- (21) Iwasaki, A.; Fujii, A.; Watanabe, T.; Ebata, T.; Makami, N. *J. Phys. Chem.* **1996**, *100*, 16053.
- (22) Morrison, R. T.; Boyd, R. N. *Organic Chemistry*, 6th ed.; Prentice Hall International: New Jersey, 1992.
- (23) Ruoff, R. S.; Klots, T. D.; Emilsson, T.; Gutowsky, H. S. *J. Chem. Phys.* **1990**, *93*, 3142.
- (24) Godfrey, P. D.; Brown, R. D.; Rodgers, F. M. *J. Mol. Struct.* **1996**, *376*, 65.
- (25) Godfrey, P. D.; Brown, R. D. *J. Am. Chem. Soc.* **1998**, *120*, 10724.
- (26) Robertson, E. G.; Hockridge, M. R.; Jelfs, P. D.; Simons, J. P. *J. Phys. Chem. A*, in press.
- (27) Vansel, S. S.; Feller, D. R. *Biochem. Pharmacol.* **1999**, *58*, 807.